Quasi-Degenerate Perturbation Theory with *General* Multiconfiguration Self-Consistent Field Reference Functions

HARUYUKI NAKANO,[1] RYUMA UCHIYAMA,[2] KIMIHIKO HIRAO[2]
[1]*Intelligent Modeling Laboratory, University of Tokyo, Tokyo 113-8656, Japan*
[2]*Department of Applied Chemistry, School of Engineering, University of Tokyo, Tokyo 113-8656, Japan*

Received 5 October 2001; Accepted 5 November 2001

Abstract: The quasi-degenerate perturbation theory (QDPT) with complete active space (CAS) self-consistent field (SCF) reference functions is extended to the general multiconfiguration (MC) SCF references functions case. A computational scheme that utilizes both diagrammatic and sum-over-states approaches is presented. The second-order effective Hamiltonian is computed for the external intermediate configurations (including virtual or/and core orbitals) by the diagrammatic approach and for internal intermediate configurations (including only active orbitals) by the configuration interaction matrix-based sum-over-states approach. The method is tested on the calculations of excitation energies of H_2O, potential energy curves of LiF, and valence excitation energies of H_2CO. The results show that the present method yields very close results to the corresponding CAS-SCF reference QDPT results and the available experimental values. The deviations from CAS-SCF reference QDPT values are less than 0.1 eV on the average for the excitation energies of H_2O and less than 1 kcal/mol for the potential energy curves of LiF. In the calculation of the valence excited energies of H_2CO, the maximum deviation from available experimental values is 0.28 eV.

 J Comput Chem 23: 1166–1175, 2002

Key words: multireference perturbation theory; quasi-degenerate perturbation theory; MC-QDPT; MC-SCF; general reference space

Introduction

The multireference perturbation theory (MRPT), based on complete active space self-consistent field (CAS-SCF) reference wave functions, has now become a basic tool for studying electronic structures of molecules and mechanisms of chemical reactions. This method takes into account both the static and dynamic electron correlation effects, and is therefore accurate, yet it is much more efficient than other multireference methods, such as the multireference configuration interaction (CI) and coupled-cluster (CC) methods.

Our multireference Møller–Plesset (MRMP) perturbation theory[1–3] and quasi-degenerate perturbation theory with multiconfiguration self-consistent field reference functions (MC-QDPT)[4,5] are perturbation theories of such a type. The MRMP PT is a multiconfiguration basis *single* reference state method based on Rayleigh–Schrödinger perturbation theory. MC-QDPT is a multiconfiguration basis *multi*-reference state method based on van Vleck PT, and therefore includes MRMP PT as a subset. Using these perturbation methods, we have clarified electronic structures of various systems and demonstrated that they are powerful tools for investigating excitation spectra and potential energy surfaces of chemical reactions.[6,7]

Although these CAS-SCF-based MRPTs are efficient, the dimension of the CAS active space, which grows very rapidly with the number of active electrons and orbitals, can be a problem. Even today, the maximum number of active orbitals that can be handled routinely in commonly used program packages is 14–16. This considerably restricts the possibility of MRPT.

To avoid the problem of the CAS dimension, we have proposed the quasi-complete active space (QCAS) SCF method[8] and MC-QDPT with QCAS-SCF wave functions as reference (hereafter we call this QCAS-QDPT).[9] QCAS is the product space of several CASs. The dimension of QCAS constructed from a set of active

Correspondence to: H. Nakano; e-mail: nakano@qcl.t.u-tokyo.ac.jp

Contract/grant sponsor: Grant-in-aid for Scientific Research on Priority Areas in Molecular Physical Chemistry (Ministry of Education, Culture, Sports, Science and Technology of Japan)

Contract/grant sponsor: Grant-in-Aid for Scientific Research (Division C), Japan Society for the Promotion of Science (to H.N.)

electrons and orbitals may be much smaller than that of CAS constructed from the same set of the electrons and orbitals. Using QCAS as reference in the perturbation theory, we may therefore extend active electrons and orbitals beyond the limit of CAS. However, it is not always possible to select an appropriate QCAS, depending on the molecular systems of interest.

In this article, we present a second-order QDPT using *general* multiconfiguration (MC) SCF wave functions as reference (hereafter, GMC-QDPT). The general MC-SCF functions are wave functions opttimized in an active space spanned by an arbitrary set of Slater determinants or configuration state functions (CSFs). We use *general* MC-SCF to distinguish it from that of specific forms like CAS-, QCAS-, and restricted active space (RAS) SCF.[10] No restriction on the form of variational space is imposed.

For MRPTs at the second-order level, the computational methods are roughly classified into two. One is the sum-over-states method based on the CI Hamiltonian matrix elements, where the intermediate (or first-order interacting) configuration functions Φ_I are constructed by single and double excitations from the reference configurations, and then the matrix elements between the reference state(s) Ψ_{Ref} and Φ_I, $\langle\Psi_{\mathrm{Ref}}|H|\Phi_I\rangle$, are computed, and finally the energy is computed as the sum over the intermediate states according to the second-order formula. The other is a diagrammatic method, where the product of the perturbation operators is computed diagrammatically without using the first-order wave functions.

An important feature of the diagrammatic method is its compactness. In fact, the second-order energy (or effective Hamiltonian) is computed simply as sums of the product of molecular integrals, coupling-coefficient, CI coefficients, and inverse of zeroth-order energy difference. It can be performed with relatively large basis sets and reference spaces. The construction of a first-order interacting space, which grows very rapidly with the number of active electrons and orbitals, is therefore unnecessary. On the other hand, an important feature of the sum-over-states method is its flexibility. The selection of the reference configuration is quite feasible in contrast to the diagrammatic method, for which a complete or quasi-complete reference is required.

The computational method for GMC-QDPT adopted here is a composite method that combines both sum-over-states and diagrammatic computational methods: the sum-over-states method is used for the excitations among active orbitals (internal excitations), while the diagrammatic method is used for the excitations including virtual or/and core orbitals (external excitations). Thus, the GMC-QDPT has both features, i.e., the compactness and flexibility.

There have been several PTs using general multiconfigurational functions: the configuration interaction by perturbation with multiconfigurational zeroth-order wave functions selected by the iterative process (CIPSI) approach by Huron et al.,[11] MROPTn with a reduced model space method by Staroverov and Davidson,[12] MRPT for (RAS and) selected active space reference functions by Celani and Werner,[13] general MRPT (based on the generalized Møller–Plesset PT of Murphy and Messmer[14]) by Grimme and Waletzke,[15] and CIPSI by Cimiraglia.[16] These methods differ formally from GMC-QDPT and from one another as well in the zeroth-order Hamiltonian or/and reference space. Computationally, most of these PTs employ the sum-over-states method, while only Cimiraglia's method[16] is diagram-based. His diagrams are defined for the vacuum states determined so as to be identical to the reference configuration that the creation and annihilation operators act on; hence, it is quite a general method. We use diagrams defined for another vacuum state, the more traditional one consisting of core orbitals.[17] These cannot be used for internal terms in the general reference case, but are quite efficient for the external terms.[4,9]

The contents of the present article is as follows: in the next section, the computational method of the second-order GMC-QDPT is described; then, the scheme is tested for the excitation energies of water molecule, potential energy curves (PECs) of the LiF molecule, and valence excitation energies of formaldehyde molecule; and in the last section the conclusions are drawn.

Method

Reference Wave Functions

The *general configuration space* (GCS) is defined by a space that is spanned by an arbitrary set of Slater determinants or CSFs. The orbitals are partitioned into three categories as in the ordinary MC-SCF method: the core orbitals are doubly occupied and the virtual orbitals are unoccupied in all the determinants/CSFs in GCS, while the active orbitals may be occupied or unoccupied. The reference wave functions used in the perturbation calculations are determined by MC-SCF (or MC-CI) using GCS as a variational space:

$$|\alpha\rangle = \sum_{A\in\mathrm{GCS}} C_A(\alpha)|A\rangle. \tag{1}$$

We call these MC-SCF wave functions *general* MC-SCF functions to distinguish them from MC-SCF functions that have specific forms.

Effective Hamiltonian to Second Order

The effective Hamiltonian up to the second order $H_{\mathrm{eff}}^{(0-2)}$ of van Vleck perturbation theory with unitary normalization is given by

$$(H_{\mathrm{eff}}^{(0-2)})_{AB} = H_{AB} + \frac{1}{2}[\langle\Phi_A^{(0)}|HR_BH|\Phi_B^{(0)}\rangle + \langle\Phi_A^{(0)}|HR_AH|\Phi_B^{(0)}\rangle] \tag{2}$$

with

$$R_A = \sum_{I\notin\mathrm{Ref}} |\Phi_I^{(0)}\rangle(E_A^{(0)} - E_I^{(0)})^{-1}\langle\Phi_I^{(0)}|, \tag{3}$$

where $\Phi_A^{(0)}$ ($\Phi_B^{(0)}$) and $\Phi_I^{(0)}$ are reference wave functions and a function in the complement space (Q) of the reference space (P), respectively, and $E_B^{(0)}$ and $E_I^{(0)}$ are zeroth-order energies of functions $\Phi_B^{(0)}$ and $\Phi_I^{(0)}$.

Adopting (state-averaged) MC-SCF (or MC-CI) wave functions α (β) as reference functions $\Phi_A^{(0)}$ ($\Phi_B^{(0)}$), which define the P space, eq. (2) becomes

$$(K_{\rm eff}^{(0-2)})_{\alpha\beta} = E_\alpha^{\rm MC\text{-}SCF}\delta_{\alpha\beta} + \frac{1}{2}\left\{\sum_{I\notin {\rm GCS}} \frac{\langle\alpha|H|I\rangle\langle I|H|\beta\rangle}{E_\beta^{(0)} - E_I^{(0)}} + (\alpha \leftrightarrow \beta)\right\}, \tag{4}$$

where I is now a determinant/CSF outside the GCS. The notation $(\alpha \leftrightarrow \beta)$ means interchange α with β from the first term in curly brackets. The complementary eigenfunctions of the MC-CI Hamiltonian and the determinants/CSFs generated by exciting electrons out of the determinants/CSFs in GCS are orthogonal to the reference functions and define the Q space. The functions in the space complementary to the P space in GCS, however, do not appear in eq. (4) because the interaction between the complementary functions and the reference functions is zero.

The GMC-QDPT computation scheme is similar to that of QCAS-QDPT.[9] We define here the corresponding CAS (CCAS) as a CAS constructed from the same active electrons and orbitals, that is, the minimal CAS that includes the reference GCS. The summation over I in eq. (4) may be divided into the summations over determinants/CSFs outside CCAS and over the determinants/CSFs outside the GCS but inside CCAS:

$$\sum_{I\notin {\rm GCS}} = \sum_{I\notin {\rm CCAS}} + \sum_{I\in {\rm CCAS}\wedge I\notin {\rm GCS}}, \tag{5}$$

then the former second order term in eq. (4) may be written as

$$(H_{\rm eff}^{(2)})_{\alpha\beta} = \sum_{I\notin {\rm CCAS}} \frac{\langle\alpha|H|I\rangle\langle I|H|\beta\rangle}{E_\beta^{(0)} - E_I^{(0)}} + \sum_{I\in {\rm CCAS}\wedge I\notin {\rm GCS}} \frac{\langle\alpha|H|I\rangle\langle I|H|\beta\rangle}{E_\beta^{(0)} - E_I^{(0)}}. \tag{6}$$

The first term in eq. (6) represents external excitations, while the latter term represents internal excitations.[9]

The external term may be further written as

$$(H_{\rm ext}^{(2)})_{\alpha\beta} = \sum_{A,B\in {\rm GCS}} C_A(\alpha)C_B(\beta)(H_{\rm ext}^{(2)})_{AB} \tag{7}$$

with

$$(H_{\rm ext}^{(2)})_{AB} = \sum_{I\notin {\rm CCAS}} \frac{\langle A|H|I\rangle\langle I|H|B\rangle}{E_B^{(0)} - E_I^{(0)} + (E_\beta^{(0)} - E_B^{(0)})}, \tag{8}$$

where $(H_{\rm ext}^{(2)})_{AB}$ is the effective Hamiltonian in the determinant/CSFs basis in the conventional QDPT except for the energy shift, $E_\beta^{(0)} - E_B^{(0)}$, in the denominator. Because the second-order diagrams do not depend on the denominator, the second-order effective Hamiltonian eq. (8) [hence, also eq. (7)] is expressed by the same diagrams as the conventional QDPT. This situation is the same as QCAS-QDPT: the diagrams and the rule for translating them into mathematical expressions is described in detail in ref. 9.

For internal terms, the diagrammatic approach may not be applied. Instead, matrix operations for the Hamiltonian matrix are used:

$$(H_{\rm int}^{(2)})_{\alpha\beta} = \mathbf{v}^T(\alpha)\cdot\mathbf{w}(\beta) \tag{9}$$

with

$$\mathbf{v}_I(\alpha) = \sum_{A\in {\rm GCS}} \langle I|H|A\rangle C_A(\alpha), \tag{10}$$

$$\mathbf{w}_I(\beta) = \sum_{B\in {\rm GCS}} \langle I|H|B\rangle C_B(\beta)/(E_\beta^{(0)} - E_B^{(0)}). \tag{11}$$

The intermediate determinants/CSFs I are constructed by exciting one or two electron(s) from the reference determinants/CSFs within the active orbital space. In general, the number of I is not large, and thus they may be managed in computer memory.

In the present implementation, we used Slater determinants rather than CSFs, differing from the original MC-QDPT.[4] Let $\{I_\alpha\}$ and $\{I_\beta\}$ be sets of alpha and beta strings appearing in the reference configurations, respectively. The reference space is defined by the beta string sets for each alpha string, $\{I_\beta[I_\alpha]\}$, and equivalently the alpha string sets for each beta string, $\{I_\alpha[I_\beta]\}$.

In the diagrammatic computation of the external terms, one-, two-, and three-body coupling coefficients (CCs) are necessary. The one-body CCs are classified into two types,

$$\langle I_\alpha|E_{pq}^\alpha|J_\alpha\rangle\langle I_\beta|J_\beta\rangle \text{ and } \langle I_\alpha|J_\alpha\rangle\langle I_\beta|E_{pq}^\beta|J_\beta\rangle,$$

the two-body CCs into three types,

$$\langle I_\alpha|E_{pq,rs}^\alpha|J_\alpha\rangle\langle I_\beta|J_\beta\rangle,\ \langle I_\alpha|J_\alpha\rangle\langle I_\beta|E_{pq,rs}^\beta|J_\beta\rangle, \text{ and } \langle I_\alpha|E_{pq}^\alpha|J_\alpha\rangle\langle I_\beta|E_{rs}^\beta|J_\beta\rangle,$$

and the three-body CCs into four types,

$$\langle I_\alpha|E_{pq,rs,tu}^\alpha|J_\alpha\rangle\langle I_\beta|J_\beta\rangle,\ \langle I_\alpha|J_\alpha\rangle\langle I_\alpha|E_{pq,rs,tu}^\alpha|J_\alpha\rangle,$$

$$\langle I_\alpha|E_{pq,rs}^\alpha|J_\alpha\rangle\langle I_\beta|E_{tu}^\beta|J_\beta\rangle, \text{ and } \langle I_\alpha|E_{pq}^\alpha|J_\alpha\rangle\langle I_\beta|E_{rs,tu}^\beta|J_\beta\rangle$$

with $J_\alpha \in \{I_\alpha\}$, $J_\beta \in \{I_\beta\}$ and

$$E_{pq,rs,\cdots}^\alpha = a_{p\alpha}^+ a_{r\alpha}^+ \cdots a_{s\alpha}a_{q\alpha}, \tag{12}$$

$$E_{pq,rs,\cdots}^\beta = a_{p\beta}^+ a_{r\beta}^+ \cdots a_{s\beta}a_{q\beta}. \tag{13}$$

Because string $J_\alpha(J_\beta)$ is determined by string $I_\alpha(I_\beta)$ and active orbital labels p and q, the one-body CCs for strings, $\langle I_\alpha|E_{pq}^\alpha|J_\alpha\rangle$ ($\langle I_\beta|E_{pq}^\beta|J_\beta\rangle$), can be stored in the computer memory in the form $J_\alpha[I_\alpha;\ p,\ q]$ ($J_\beta[I_\beta;\ p,\ q]$). The perturbation calculation for three-body CCs, $\langle I_\alpha|E_{pq,rs}^\alpha|J_\alpha\rangle\langle I_\beta|E_{tu}^\beta|J_\beta\rangle$, for example, is done as follows:

```
Loop over I_α
  Make all non-zero ⟨I_α|E^α_{pq,rs}|J_α⟩ for I_α
  Loop over I_β[I_α]
    Loop over t and u
    If J_β[I_β; t, u] ≠ 0 and J_β[I_β; t, u] ∈ {I_β[J_α]},
                                                  then
       do 3-body PT calculations for
                                  ⟨I_α|E^α_{pq,rs}|J_α⟩⟨I_β|E^β_{tu}|J_β⟩
```

```
    end loop t and u
  end loop I_β[I_α]
end loop I_α
```

The other terms can be computed similarly.

Other ways for computing CCs may be possible. However, because the PT calculation parts are more time consuming, the difference is not critical.

The one- and two-body CCs computed in the same manner are used for the CI based calculation for the internal terms. The vectors $\mathbf{v}_I$ in eq. (9) are computed as σ-vectors using strings. (Note that other efficient methods[18,19] are known for the σ-vector part of the algorithm.)

Applications

Excitation Energies of H_2O

First, we applied GMC-QDPT to the excitation energies of water molecule.

The single and double excitation CI molecular structure reported in the paper by Laidig et al.[20] was used. The basis set was Dunning's double zeta basis set.[21]

The reference space was constructed from eight electrons and eight orbitals, $(a_1, a_2, b_1, b_2) = (4, 0, 2, 2)$, where the numbers in the parenthesis denote the numbers of active orbitals in each irreducible representation. The construction is similar to parent configuration (PC) CI, that is, by exciting one and two electrons within active orbitals from the parent configurations listed as follows:

$^1A_1$states: $\cdots n^2$(HF); $3a_1(\sigma) \rightarrow 4a_1(\sigma^*)$; $1b_1(\sigma) \rightarrow 2b_1(\sigma^*)$
$^3A_1$states: $3a_1(\sigma) \rightarrow 4a_1(\sigma^*)$; $1b_1(\sigma) \rightarrow 2b_1(\sigma^*)$
$^{1,3}A_2$states: $n \rightarrow 2b_2(\pi^*)$
$^{1,3}B_1$states: $n \rightarrow 4a_1(\sigma^*)$
$^{1,3}B_2$states: $1b_1(\sigma) \rightarrow 4a_1(\sigma^*)$; $3a_1(\sigma) \rightarrow 2b_2(\pi^*)$

The CAS for comparison is CAS(8, 8). All the calculations were done in each symmetry: the numbers of states were three ($^1A_1$), two ($^3A_1$ and $^{1,3}B_2$), and one ($^{1,3}A_2$ and $^{1,3}B_1$).

Tables 1 and 2 show the results of GMC-QDPT and its reference MC-SCF, the original MC-QDPT (hereafter CAS-QDPT) and its reference CAS-SCF, and full CI method. The full CI numbers were taken from refs. 22 and 23. Figures 1 and 2 are plots of the difference from the full CI values at reference (MC-SCF and CAS-SCF) and PT (GMC- and CAS-QDPT) levels. It can be seen from Figures 1 and 2 that the results of the two methods (MC-SCF and CAS-SCF) at reference level are quite similar, and that the same is true of the results of the two (GMC- and CAS-QDPT) at PT level, indicating that the present method well reproduces the CAS results. The deviations are 0.04 (0.06) eV on average and 0.06 (0.07) eV at maximum at PT (reference) level. Moreover, GMC-QDPT gave close excitation energies also to full CI. The excitation energies for this very small basis set of a small molecule are very good already at the reference level: the error is 0.20 eV on average and 0.40 eV at maximum. The PT improved the results further: the average and maximum errors are 0.05 and 0.14 eV, respectively.

Potential Energy Curves of LiF

The second example is the calculation of the PECs of the two lowest $^1\Sigma^+$ states of the LiF molecule. In the diabatic picture, one of the $^1\Sigma^+$ states is ionic and the other state is covalent. In the equilibrium structure region the ionic state is lower in energy (the ground state), while at the dissociation limit the covalent state is lower. The two potential curves therefore show avoided-crossing in the middle in the adiabatic picture. This system was examined in a previous article of QCAS-QDPT[9] as well as CAS-QDPT.[4] In the present article, we compare GMC-QDPT results with CAS- and QCAS-QDPT results.

The basis set used was 6-311++G(3*df*, 3*pd*).[24] The reference spaces were made by exciting one and two electrons from two parent configurations: the Hartree–Fock and $4\sigma \rightarrow 5\sigma^*$ excitation configurations. The CAS and QCAS used for comparison were CAS(6, 9), and QCAS[$(2, 3)^3$], respectively, where in QCAS the division of the nine orbitals were $\{4\sigma$–$6\sigma\}$, $\{1\pi$–$3\pi\}$, and $\{1\pi'$–$3\pi'\}$. The dimension of GCS was 241, and those of CAS and QCAS were 1812 and 729 (in Slater determinant basis; with symmetry), respectively. The 1σ orbital corresponding to F(1*s*) was frozen in the perturbation calculations.

Results are shown in Figures 3–5. Figure 3 shows PECs at the MC- and CAS-SCF levels, and Figure 4 shows PECs at the GMC- and CAS-QDPT levels. The errors of the reference function (MC-SCF/CAS-SCF) level and perturbation theory (GMC-QDPT/CAS-QDPT) level are plotted in Figure 5. Figure 6 shows the same information as Figure 3 in ref. 9 for comparison, that is, the errors of QCAS-SCF and QCAS-QDPT from CAS-SCF and CAS-QDPT, respectively.

The error patterns of the MC-SCF and GMC-QDPT in Figure 5 are very similar to that of the QCAS-SCF and QCAS-QDPT in Figure 6, respectively. As in the case of the QCAS-SCF, the MC-SCF curves have systematic errors from the CAS-SCF results depending on the nature of the states: about 4 kcal/mol for the ionic state (in the diabatic picture; lower the near equilibrium structure, higher at the dissociation limit) and about 2.5 kcal/mol for the covalent state. These are recovered well by GMC-QDPT. At this level, the errors from CAS-QDPT are less than 1 kcal/mol for both states. The dimension of GCS, 241, is about one-third of QCAS, 729, yet the performance is very similar. We can therefore say that GMC-QDPT is more efficient than QCAS-QDPT with respect to the reference dimension.

Valence Excitation Energies for Formaldehyde

The final example is the calculation of valence excitation energies for formaldehyde molecule. Calculations on formaldehyde were carried out at the ground state experimental geometry[25] (i.e., r(CO) = 1.203 Å, r(CH) = 1.099 Å, and θ(HCH) = 116.5 degree). The basis set used was Dunning's cc-pVTZ.[26]

Five reference spaces were constructed from 8 electrons, 16 $[(a_1, a_2, b_1, b_2) = (7, 1, 3, 5)]$, 18 [=(7, 1, 4, 6)], 20 [=(8, 1, 5, 6)], 22 [=(8, 2, 5, 7)], and 24 orbitals [=(9, 2, 6, 7)], by

Table 1. Singlet Excitation Energies of H_2O.

State	Method	Total Energy/ Hartree	Excitation Energy/eV	Error[a]/eV
1^1A_1	CAS-SCF	−76.088595	—	—
	MC-SCF	−76.085280	—	—
	CAS-QDPT	−76.151288	—	—
	GMC-QDPT	−76.152957	—	—
	Full CI[b]	−76.157866	—	—
2^1A_1	CAS-SCF	−75.684354	11.00	0.16
	MC-SCF	−75.682254	10.97	0.13
	CAS-QDPT	−75.755914	10.76	−0.08
	GMC-QDPT	−75.756342	10.79	−0.05
	Full CI[c]	−75.759512	10.84	—
3^1A_1	CAS-SCF	−75.378624	19.32	0.26
	MC-SCF	−75.373273	19.37	0.31
	CAS-QDPT	−75.454840	18.95	−0.11
	GMC-QDPT	−75.457734	18.92	−0.14
	Full CI[c]	−75.457584	19.06	—
1^1A_2	CAS-SCF	−75.697467	10.64	−0.16
	MC-SCF	−75.696525	10.58	−0.22
	CAS-QDPT	−75.754637	10.79	−0.01
	GMC-QDPT	−75.754313	10.85	0.05
	Full CI[c]	−75.761050	10.80	—
1^1B_1	CAS-SCF	−75.781645	8.35	−0.35
	MC-SCF	−75.780198	8.30	−0.40
	CAS-QDPT	−75.831630	8.70	0.00
	GMC-QDPT	−75.831460	8.75	0.05
	Full CI[c]	−75.838288	8.70	—
1^1B_2	CAS-SCF	−75.591791	13.52	0.25
	MC-SCF	−75.591108	13.45	0.18
	CAS-QDPT	−75.665094	13.23	−0.04
	GMC-QDPT	−75.665270	13.27	0.00
	Full CI[c]	−75.670141	13.27	—
2^1B_2	CAS-SCF	−75.502941	15.94	−0.02
	MC-SCF	−75.502138	15.87	−0.09
	CAS-QDPT	−75.564328	15.97	0.01
	GMC-QDPT	−75.564317	15.94	−0.02
	Full CI[c]	−75.571512	15.96	—

[a]Differences from full CI values.
[b]Ref. 22.
[c]Ref. 23.

exciting one and two electrons from the following parent configurations:

$^1A_1$states: $\cdots n^2$(HF); $\pi \rightarrow \pi^*$; $n \rightarrow \sigma^*$
$^3A_1$states: $\pi \rightarrow \pi^*$; $n \rightarrow \sigma^*$
$^{1,3}A_2$states: $n \rightarrow \pi^*$; $1b_2(\sigma) \rightarrow \pi^*$
$^{1,3}B_1$states; $5a_1(\sigma) \rightarrow \pi^*$
$^{1,3}B_2$states: $n \rightarrow 6a_1(\sigma^*)$.

The dimensions of the reference spaces, for example, in singlet A_1 were 3045, 4121, 5349, 6833, and 8413 for 16, 18, 20, 22, and 24 active orbitals, respectively: the dimension increase like an arithmetic progression. The corresponding dimensions of symmetry-adapted CASs were 828 720 (n_{act} = 16), 2 342 000 (=18), 5 871 601 (=20), 13 380 441 (=22), and 28 234 186 (=24). This increases much more rapidly than the GCS cases. All the calculations were done in each symmetry.

The results are summarized in Tables 3 and 4. The calculations with CAS-SCF and CAS-QDPT are far too large to be done. We, therefore, compare the results with available experimental results and some recent theoretical results, i.e., MR-CI results by Hachey et al.,[27] the second-order complete active space perturbation theory (CASPT2) calculations by Merchán and Roos,[28] and the equation of motion coupled cluster (EOM-CC) calculations by Gwaltney et al.[29]

As can be computed from Table 3, the maximum differences in excitation energy for the largest three (two) numbers of active orbitals is 0.09 (0.05) eV. We can therefore consider that the excitation energies at the MC-SCF level are almost converged values for the change of the active orbital numbers. However, the

Table 2. Triplet Excitation Energies of H_2O.

State	Method	Total Energy/ Hartree	Excitation Energy/eV	Error[a]/eV
1^3A_1	CAS-SCF	−75.728151	9.81	−0.01
	MC-SCF	−75.726996	9.75	−0.07
	CAS-QDPT	−75.792925	9.75	−0.07
	GMC-QDPT	−75.793762	9.77	−0.05
	Full CI[b]	−75.797174	9.82	—
2^3A_1	CAS-SCF	−75.504622	15.89	−0.12
	MC-SCF	−75.503037	15.84	−0.17
	CAS-QDPT	−75.565397	15.94	−0.07
	GMC-QDPT	−75.565677	15.98	−0.03
	Full CI[b]	−75.569523	16.01	—
1^3A_2	CAS-SCF	−75.715650	10.15	−0.13
	MC-SCF	−75.714584	10.09	−0.19
	CAS-QDPT	−75.773175	10.29	0.01
	GMC-QDPT	−75.773149	10.34	0.06
	Full CI[b]	−75.779926	10.28	—
1^3B_1	CAS-SCF	−75.811322	7.55	−0.35
	MC-SCF	−75.809834	7.50	−0.40
	CAS-QDPT	−75.861143	7.90	0.00
	GMC-QDPT	−75.860964	7.95	0.05
	Full CI[b]	−75.867507	7.90	—
1^3B_2	CAS-SCF	−75.650702	11.92	0.05
	MC-SCF	−75.649829	11.85	−0.02
	CAS-QDPT	−75.717678	11.80	−0.07
	GMC-QDPT	−75.718368	11.83	−0.04
	Full CI[b]	−75.721626	11.87	—
2^3B_2	CAS-SCF	−75.571768	14.06	−0.16
	MC-SCF	−75.570499	14.01	−0.21
	CAS-QDPT	−75.631462	14.15	−0.07
	GMC-QDPT	−75.631627	14.19	−0.03
	Full CI[b]	−75.635841	14.22	—

[a]Differences from full CI values.
[b]Ref. 23.

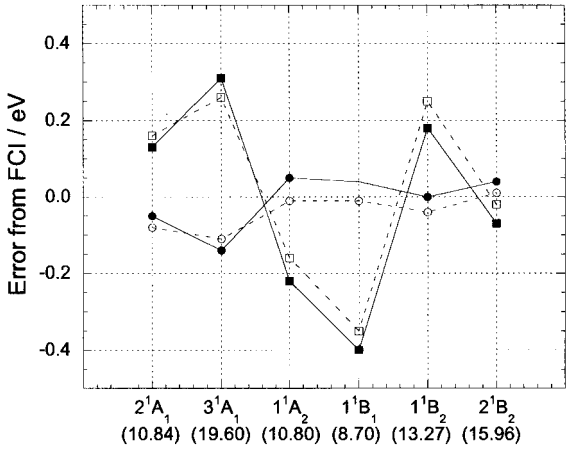

Figure 1. Error from full CI results in singlet excitation energies of H_2O (the values in the parentheses are full CI excitation energies in eV).

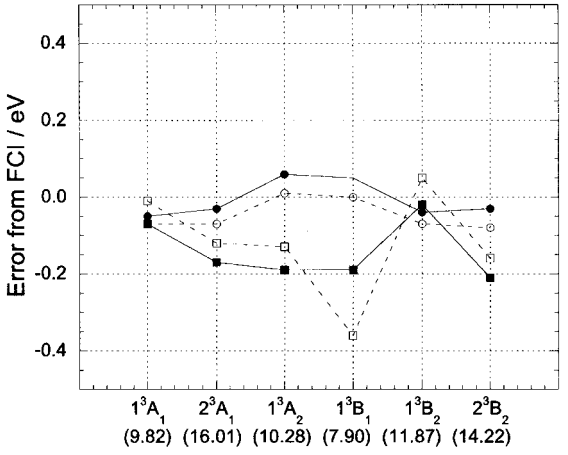

Figure 2. Error from full CI results in triplet excitation energies of H_2O (the values in the parentheses are full CI excitation energies in eV).

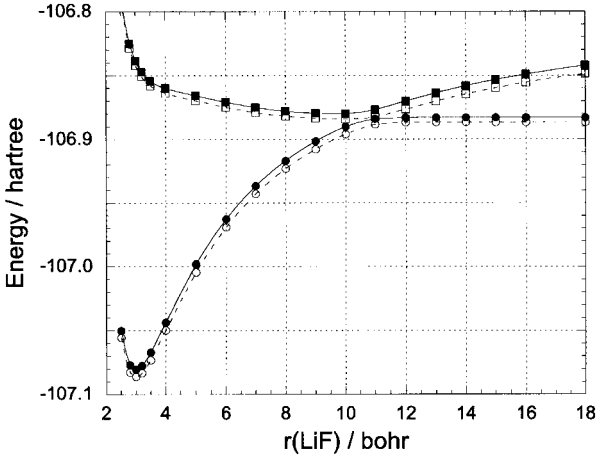

Figure 3. The MC-SCF (●, ■) and CAS-SCF (○, □) potential energy curves of the two lowest $^1\Sigma^+$ states of LiF.

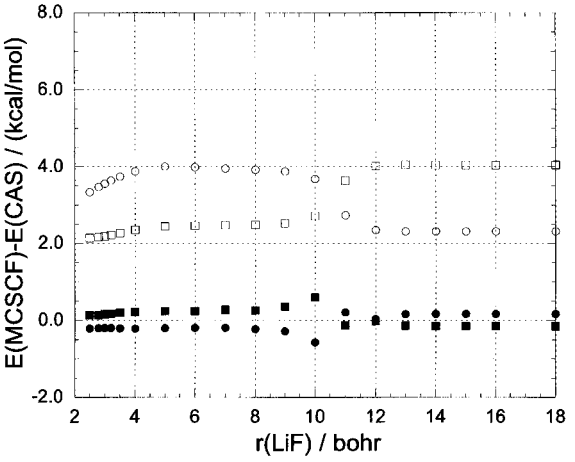

Figure 5. The energy differences of the two lowest $^1\Sigma^+$ states of LiF between GMC- and CAS-QDPT (the symbols ● and ■ are for the ground and excited states, respectively) and between MC- and CAS-SCF (○, □ for the ground and excited state, respectively).

agreement with the experimental values is not as good: the error is 0.32 eV on average and 0.80 eV at maximum.

At the GMC-QDPT level, the excitation energies are also almost converged (though the differences are a little larger than those at MC-SCF level are). Compared to the reference MC-SCF level, the results are somewhat improved. The error from the experimental value was reduced to 0.11 eV on average and 0.28 eV at maximum.

Theoretical results by multireference methods (MRCI and CASPT2) and EOM-CC are also available for several low-lying states. Harchey et al.[27] presented the MRCI results for four singlet states [1^1A_2(4.05 eV), 1^1B_1(9.35 eV), and 2^1A_1(9.60 eV) states], Merchén et al.[28] reported the CASPT2 results for three singlet and two triplet states [1^1A_2 (3.91 eV), 1^1B_1 (9.09 eV), 2^1A_1 (9.77 eV), 1^3A_2 (3.48 eV), and 2^3A_1 (5.99 eV) states], and Gwaltney et al.[29] gave the EOM-CC results for four singlet states [1^1A_2 (3.98 eV), 1^1B_1 (9.33 eV), 2^1A_1 (9.47 eV), and 2^1A_2 (10.38 eV) states]. These values are all close to the GMC-QDPT values, supporting the present results.

Before these studies, many works were conducted, three of which are listed in Table 4. Hadad et al.[30] calculated higher excited states with CIS-MP2. The computed excitation energies are too high, except for the 2^1A_1 state, compared to the other results. The CIS method overestimates excitation energies in general, and this defect of CIS carried over to the MP2 level. Head-Gordon et al.[31] calculated three lowest singlet excited states with CCSD in an article that estimated the doubles correction for CIS. The CCSD results were in good agreement with GMC-QDPT, although the 2^1A_1 state is a little lower. The SAC-CI method[32] was made for higher states, and the results reproduced experimental values well.

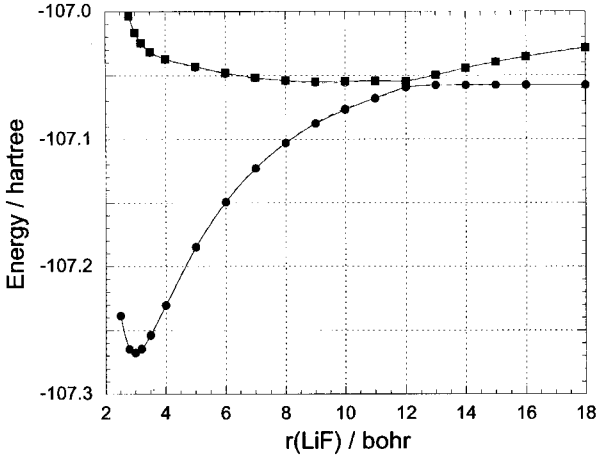

Figure 4. The GMC-QDPT (●, ■) and CAS-QDPT (●, □) potential energy curves of the two lowest $^1\Sigma^+$ states of LiF.

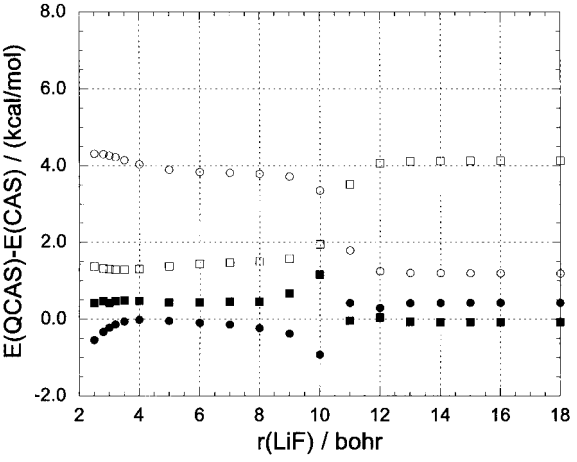

Figure 6. The energy differences of the two lowest $^1\Sigma^+$ states of LiF between QCAS- and CAS-QDPT (the symbols ● and ■ are for the ground and excited states, respectively) and between QCAS- and CAS-SCF (○, □ for the ground and excited state, respectively).

Table 3. Valence Excitation Energies of H_2CO (eV).

State	Orbital Picture	MC-SCF (8, 16)	MC-SCF (8, 18)	MC-SCF (8, 20)	MC-SCF (8, 22)	MC-SCF (8, 24)	GMC-QDPT (8, 16)	GMC-QDPT (8, 18)	GMC-QDPT (8, 20)	GMC-QDPT (8, 22)	GMC-QDPT (8, 24)	Experiment[a]
$^1A_1$	$\pi \rightarrow \pi^*$; $n \rightarrow \sigma^*$	10.07	10.03	10.03	10.02	10.02	9.66	9.67	9.72	9.72	9.72	
	$n \rightarrow \sigma^*$; $\pi \rightarrow \pi^*$	11.01	11.01	11.00	11.03	11.01	10.65	10.63	10.65	10.63	10.64	10.70
$^1A_2$	$n \rightarrow \pi^*$	4.32	4.43	4.27	4.25	4.22	4.04	4.02	4.01	4.02	4.08	4.07
	$1b_2(\sigma) \rightarrow \pi^*$	10.96	11.16	10.97	10.98	10.94	10.30	10.34	10.33	10.37	10.43	
$^1B_1$	$5a_1(\sigma) \rightarrow \pi^*$	9.63	9.89	9.82	9.81	9.80	9.31	9.24	9.26	9.20	9.28	9.00
$^1B_2$	$n \rightarrow 6a_1(\sigma^*)$	7.73	8.16	8.22	8.32	8.31	8.31	8.23	8.41	8.45	8.45	
$^3A_1$	$\pi \rightarrow \pi^*$; $n \rightarrow \sigma^*$	6.18	6.28	6.19	6.13	6.11	6.13	6.13	6.18	6.17	6.18	6.00
	$n \rightarrow \sigma^*$; $\pi \rightarrow \pi^*$	9.66	9.64	9.70	9.74	9.75	9.60	9.61	9.62	9.62	9.62	
$^3A_2$	$n \rightarrow \pi^*$	3.84	3.95	3.78	3.75	3.71	3.63	3.58	3.58	3.61	3.63	3.50
	$1b_2(\sigma) \rightarrow \pi^*$	10.52	10.68	10.52	10.52	10.47	10.04	10.03	10.02	10.07	10.10	
$^3B_1$	$5a_1(\sigma) \rightarrow \pi^*$	8.78	9.02	8.92	8.91	8.90	8.45	8.41	8.39	8.27	8.50	8.50
$^3B_2$	$n \rightarrow 6a_1(\sigma^*)$	7.36	7.79	7.85	7.95	7.94	7.89	7.80	7.99	8.02	8.07	

[a]References in Refs. 27 and 32.

These results are also close to the GMC-QDPT results except for the $2A_2$ singlet and triplet states.

Overall, the GMC-QDPT reproduces available experimental results and is also close to the results of highly correlated methods.

Internal-Term Contribution

In the previous QCAS-QDPT article, we pointed out the importance of the internal-term contribution. For the QCAS-SCF reference functions, the internal terms are essential for a balanced description of relative energies or potential energy surfaces, even though the contribution is small. Because the GMC-QDPT includes the QCAS-QDPT, the neglect of the internal terms is not justified in general. However, it is useful to check the significance of them in the present choice of reference MC-SCF functions, that is, parent configurations plus single and double (PC-SD) excitations. In this case, the internal excitations correspond to triple and quadruple excitations from parent configurations. Figure 7 shows the potential energy curves (PECs) of the lowest two $^1\Sigma^+$ states of LiF. The curves plotted with filled (open) symbols are GMC-QDPT PECs without (with) the internal term contribution. Although the energy without the internal term contribution is higher than that with the full-term contribution along the entire curves, the deviation is almost constant in both states: 2.5–3.0 kcal/mol. In other words, even without the internal term contribution, the GMC-QDPT almost reproduces the full GMC-QDPT results. Table 5 summarizes the valence excitation energies of H_2CO calculated by GMC-QDPT without the internal term contribution and

Table 4. Valence Excitation Energies of H_2CO (eV).

State	Orbital Picture	MC-SCF (8, 24)	GMC-QDPT (8.24)	Experiment	MRCI[a]	CASPT2[b]	EOM-CC[c]	CCSD[d]	CIS-MP2[e]	SAC-CI[f]
$^1A_1$	$\pi \rightarrow \pi^*$, $n \rightarrow \sigma^*$	10.02	9.72		9.60	9.77	9.47	9.27	9.19	—
	$n \rightarrow \sigma^*$, $\pi \rightarrow \pi^*$	11.01	10.64	10.70						10.83
$^1A_2$	$n \rightarrow \pi^*$	4.22	4.08	4.07	4.05	3.91	3.98	3.95	4.58	4.16
	$1b_2(\sigma) \rightarrow \pi^*$	10.94	10.43				10.38		10.08	11.19
$^1B_1$	$5a_1(\sigma) \rightarrow \pi^*$	9.80	9.28	9.00	9.35	9.09	9.33	9.26	9.97	9.49
$^1B_2$	$n \rightarrow 6a_1(\sigma^*)$	8.31	8.45							
$^3A_1$	$\pi \rightarrow \pi^*$; $n \rightarrow \sigma^*$	6.11	6.18	6.00		5.99			6.72	6.10
	$n \rightarrow \sigma^*$; $\pi \rightarrow \pi^*$	9.75	9.62							
$^3A_2$	$n \rightarrow \pi^*$	3.71	3.63	3.50		3.48			4.15	3.70
	$1b_2(\sigma) \rightarrow \pi^*$	10.47	10.10						10.52	10.80
$^3B_1$	$5a_1(\sigma) \rightarrow \pi^*$	8.90	8.50	8.50					9.18	8.52
$^3B_2$	$n \rightarrow 6a_1(\sigma^*)$	7.94	8.07							

[a]Ref. 27.
[b]Ref. 28.
[c]Ref. 29.
[d]Ref. 30.
[e]Ref. 31.
[f]Ref. 32.

that with the full-term contribution. The excitation energies predicted by both methods are close. The average and maximum deviations are 0.10 and 0.30 eV, respectively.

These results indicate that, for the present choice of reference, the internal term contribution is not as important in contrast to the QCAS-QDPT case. This may be useful for the PC-SD-type reference, because (1) the external terms are computed in the same manner as the original MC-QDPT, differing only in the number of coupling coefficients, hence simple; and (2) in the internal term computation, the construction of the SD space is time consuming in some cases.

Concluding Remarks

The second-order QDPT with CAS- or QCAS-SCF reference functions was extended to the general MC-SCF reference functions case, i.e., GMC-QDPT. There is no longer any restriction on the form of the reference space. It can treat more active orbitals and electrons than a CAS reference PT, and thus is applicable to larger systems, and it can avoid unphysical multiple excited configurations, which are often responsible for the intruder state problem.

A computational scheme that utilizes both diagrammatic and CI matrix-based sum-over-states approaches was presented. The second-order GMC-QDPT effective Hamiltonian is computed for the external (outside CAS) and internal (inside CAS) intermediate configurations separately. For external intermediate configuration, the diagrammatic approach is used, which has been used for CAS- and QCAS-QDPT. The diagrams are identical to those of CAS- and QCAS-QDPT; only the computational scheme of coupling coefficients is different. For the internal intermediate configurations, a CI matrix-based method is used. The vectors used belong to MR-SD-CI space within active orbitals, and therefore small enough to be easily treatable.

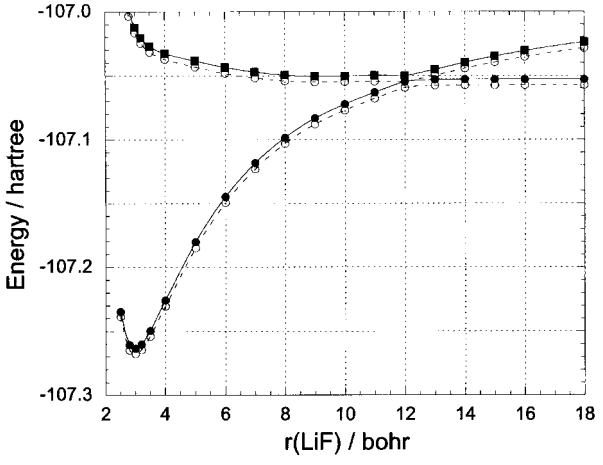

Figure 7. The GMC-QDPT potential energy curves of the two lowest $^1\Sigma^+$ states of LiF: the curves of GMC-QDPT without the internal term contribution (the symbols ● and ■ are for the ground and excited states, respectively) and those of full GMC-QDPT (○, □ for the ground and excited state, respectively).

Table 5. Valence Excitation Energies of H_2CO Computed Without and With Internal Term Contribution (eV).

State	Orbital Picture	No Internal Terms[a]	Full Terms[a]	Difference
$^1A_1$	$\pi \rightarrow \pi^*$, $n \rightarrow \sigma^*$	9.78	9.72	0.06
	$n \rightarrow \sigma^*$, $\pi \rightarrow \pi^*$	10.76	10.64	0.12
$^1A_2$	$n \rightarrow \pi^*$	4.15	4.08	0.07
	$1b_2(\sigma) \rightarrow \pi^*$	10.73	10.43	0.30
$^1B_1$	$5a_1(\sigma) \rightarrow \pi^*$	9.16	9.28	−0.12
$^1B_2$	$n \rightarrow 6a_1(\sigma^*)$	8.46	8.45	0.01
$^3A_1$	$\pi \rightarrow \pi^*$; $n \rightarrow \sigma^*$	6.06	6.18	−0.12
	$n \rightarrow \sigma^*$; $\pi \rightarrow \pi^*$	9.68	9.62	0.06
$^3A_2$	$n \rightarrow \pi^*$	3.67	3.63	0.04
	$1b_2(\sigma) \rightarrow \pi^*$	10.30	10.10	0.20
$^3B_1$	$5a_1(\sigma) \rightarrow \pi^*$	8.46	8.50	−0.04
$^3B_2$	$n \rightarrow 6a_1(\sigma^*)$	8.11	8.07	0.04

[a]Results for the (8, 24) reference space.

The method was tested on excitation energies of the water molecule, the potential energy curves of the LiF molecule, and the valence excitation energies of the formaldehyde molecule. The present method yields very close results to the corresponding CAS-SCF reference MC-QDPT results and the available experimental values. The deviations from CAS-QDPT values are less than 0.1 eV on the average for the excitation energies of water and less than 1 kcal/mol for the potential energy curves of LiF. In the calculation of the valence excited energies of formaldehyde, the maximum deviation from available experimental values was 0.28 eV.

It is also shown that the internal term contribution is not important if the reference with the parent configurations plus single and double excitations (PC-SD) is used. This feature is useful because it illustrates the possibility that we can omit the time-consuming internal terms.

The construction of the reference space used here, PC-SD, is an example of a general reference space. Finally, it is emphasized that GMC-QDPT can be applied to any reference space. The application to other types of reference space will be shown in forthcoming articles.

Acknowledgments

The authors thank Professor Mark S. Gordon (Iowa State University) for valuable discussions.

References

1. Hirao, K. Chem Phys Lett 1992, 190, 374.
2. Hirao, K. Chem Phys Lett 1992, 196, 397.
3. Hirao, K. Intern J Quantum Chem 1992, S26, 517.

4. Nakano, H. J Chem Phys 1993, 99, 7983.
5. Nakano, H. Chem Phys Lett 1993, 207, 372.
6. Nakano, H.; Yamanishi, M.; Hirao, K. Trends Chem Phys 1997, 6, 167.
7. Nakano, H.; Nakajima, T.; Tsuneda, T.; Hirao, K. J Mol Struct (Theochem) 2001, 573, 91.
8. Nakano, H.; Hirao, K. Chem Phys Lett 2000, 317, 90.
9. Nakano, H.; Nakatani, J.; Hirao, K. J Chem Phys 2001, 114, 1133.
10. Olsen, J.; Roos, B. O.; Jørgensen, P.; Jensen, H. J. Aa. J Chem Phys 1988, 89, 2185.
11. Huron, B.; Malrieu, J.-P.; Rancurel, P. J Chem Phys 1973, 58, 5745.
12. Staroverov, V. N.; Davidson, E. R. Chem Phys Lett 1998, 296, 435.
13. Celani, P.; Werner, H.-J. J Chem Phys 2000, 112, 5546.
14. Murphy, R. B.; Messmer, R. P. Chem Phys Lett 1991, 183, 443.
15. Grimme, S.; Waletzke, M. Phys Chem Chem Phys 2000, 2, 2075.
16. Cimiraglia, R. J Chem Phys 1985, 83, 1746.
17. Lindgren, I.; Morrison, J. Atomic Many-Body Theory, 2nd ed.; Springer-Verlag: New York, 1982.
18. Povill, A.; Rubio, J.; Illas, F. Theor Chim Acta 1992, 82, 229.
19. Povill, A.; Rubio, J. Theor Chim Acta 1995, 92, 305.
20. Laidig, W. D.; Saxe, P.; Schaefer, H. F., III. J Chem Phys 1980, 73, 1765.
21. Dunning, T. H., Jr. J Chem Phys 1970, 53, 2823.
22. Saxe, P.; Schaefer, H. F., III; Handy, N. C. Chem Phys Lett 1981, 79, 202.
23. Hirao, K. Chem Phys Lett 1993, 201, 59.
24. Krishnan, R.; Binkley, J. S.; Seeger, R.; Pople, J. A. J Chem Phys 1980, 72, 650.
25. Yamada, K.; Nakagawa, T.; Morino, Y. J Mol Spectrosc 1971, 38, 70.
26. Dunning, T. H., Jr. J Chem Phys 1989, 90, 1007.
27. Hachey, M. R. J.; Bruna, P. J.; Grein, F. J Phys Chem 1995, 99, 8050.
28. Merchán, M.; Roos, B. O. Theor Chim Acta 1995, 92, 227.
29. Gwaltney, S. R.; Bartlett, R. J. Chem Phys Lett 1995, 241, 26.
30. Hadad, C. M.; Foresman, J. B.; Wiberg, K. B. J Phys Chem 1993, 97, 4293.
31. Head–Gordon, M.; Rico, R. J.; Oumi, M.; Lee, T. J. Chem Phys Lett 1994, 219, 21.
32. Nakatsuji, H.; Ohta, K.; Hirao, K. J Chem Phys 1981, 75, 2952.